

## Microstructure of textured $\text{YBa}_2\text{Cu}_3\text{O}_{7-\delta}$ prepared by the melted zone in magnetic field: texturation mechanism

D. Bourgault<sup>a</sup>, J.M. Barbut<sup>b</sup>, J. Ayache<sup>c</sup>, D. Chateigner<sup>d</sup>, R. Tournier<sup>a</sup>, F.J. Gotor<sup>e</sup>, C. Bahezre<sup>c</sup>, P. Germi<sup>d</sup> and M. Pernet<sup>d</sup>.

<sup>a</sup>Laboratoire Matformag - CNRS 38042 Grenoble cedex 9, France.

<sup>b</sup>Merlin Gerin, Centre de Recherche A2, 38050 Grenoble cedex, France.

<sup>c</sup>Laboratoire Physique des Matériaux, 92495 Meudon Cedex, France.

<sup>d</sup>Laboratoire de Cristallographie, CNRS- UJF BP 166, 38042 Grenoble cedex 9, France.

<sup>e</sup>CRPHT CNRS 45071 Orléans cedex, France.

A zone melting set-up with a magnetic field perpendicular to the temperature gradient is used in order to optimize (a, b) plane alignment and thus critical current densities. Large samples with high  $J_c$  values in magnetic fields at 77K are obtained. These studies are carried out by optical microscopy, analytical transmission electron microscopy and X ray diffraction pole figures. Our results indicate that crystallite misorientation within a single domain does not exceed  $10^\circ$ . The application of a magnetic field of 5 T imposes the c-axis orientation during grain growth. Indeed, we observe an intergrain dispersion much smaller than  $40^\circ$  with respect to the magnetic field direction. The 123 matrix contains large amounts of unoriented 211 inclusions which are of different size.

### 1. INTRODUCTION

Very large critical current densities have been obtained in magnetically melt textured (MMT)  $\text{YBa}_2\text{Cu}_3\text{O}_{7-\delta}$  ceramic material [1]. The use of a zone melting set-up to texture superconducting materials should allow the fabrication of large size bar samples in a continuous process [2,3], but this method has several shortcomings. In this paper, we report results obtained in a YBCO large textured sample using an experimental set-up which combines the effects of both thermal gradient and magnetic field ( $H = 5\text{T}$ ).

### 2. EXPERIMENTAL

Texturation of  $\text{YBa}_2\text{Cu}_3\text{O}_{7-\delta}$  material is insured by the displacement of the bar sample through the hot zone of the furnace, whereas the sample c-axis orientation is directed along the magnetic field [4]. The standard 4 points technique with an electric field criterion of  $10 \mu\text{V}/\text{cm}$  has been used for d.c. transport critical current measurements at 77 K and in magnetic fields as high as 8 teslas. The magnetic field is applied perpendicularly to the direction of current flow while the sample can be rotated, thus varying the angle  $\Theta$  with a precision higher than  $1^\circ$ .  $\Theta$  is the angle between the measuring magnetic field and a face of the bar perpendicular to the direction of the annealing field. The bar has then been cut and polished for optical microscopy, transmission

electron microscopy and X ray diffraction pole figures, along two perpendicular faces. One, B (of normal n), is cut parallel to the  $(H, \nabla T)$  plane, while the other, A, is parallel to the  $(n, \nabla T)$  plane.

### 3. RESULTS AND DISCUSSION

#### 3.1. Transport properties

Figure 1 shows the angular dependence of the transport critical current at 77 K for different values of the magnetic field.

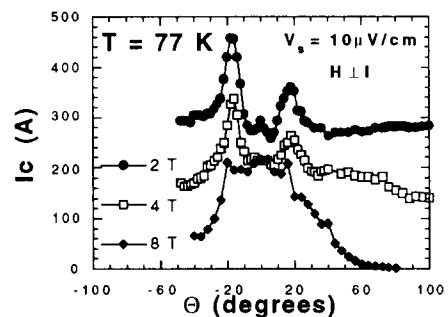


Figure 1. Angular dependence of the transport critical current in fields of 2 up to 8 teslas at 77 K.

Several sharp peaks are observed in the  $\Theta = 0^\circ$  region. They correspond to intrinsic pinning by the layered structure of several textured domains. The presence of two peaks proves the existence of two

different textured domains which are slightly misaligned within the material ( $\pm 20^\circ$ ). This phenomenon is indicative of a good orientation of the material, which is attributed to the application of a magnetic field during the annealing.

We must note here that the transport critical current is larger than 1000 A (the limit of our current source) at  $H = 0$  T [4].

### 3.2. Quantitative determination of the texture

The texture of the bar was analysed by X-ray diffraction pole figures [5] on faces A and B (20mm long and 3mm large). Three zones at L/3, L/2 and 2L/3 of each face were analysed, the irradiated volume on each zone being of the order of  $1 \times 2 \text{ mm}^2 \times 10 \mu\text{m}$ .

Three-dimensional textured domains distributed within the sample were observed in  $\{104\}_{123}$  pole figures. The dispersion of the crystallites inside the domains is ascribed in a cone of  $\approx 10^\circ$  aperture at 15% of the maximal intensity, but the poles are not of systematic geometry. Two domains are currently observed for each zone, which are dispersed at maximum by  $15^\circ$  with respect to each other. As shown in figure 2a, which represents 3 zones of A, the (a, b) planes can rotate around the bisector of  $n$  and  $\nabla T$  with a dispersion of the  $c$ -axis much smaller than  $40^\circ$  with respect to the magnetic field direction.

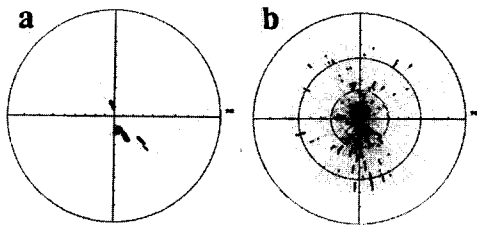


Figure 2. a)  $\{005\}_{123}$  of the L/3, L/2 and 2L/3 zones. b)  $\{113\}_{211}$  pole figure.

The 2L/3 zones of A and B are coherent with each other for the  $\{005\}$  poles, in such a way that this particular region of the bar can be considered as one single domain, whereas this is not the case for the L/2 and L/3 zones. In the L/2 zone, the domains observed on faces A and B are oriented with their  $c$ -axes at  $\approx -20^\circ$  and  $\approx 20^\circ$  from H. This is in good agreement with transport critical current measurements realized at this point (Figure 1).

Finally, Figure 2b shows the  $\{113\}_{211}$  pole

figure where no orientation of the green phase induced by this method is visible.

### 3.3. Microstructure

Optical microscopy (OM) observations are in agreement with pole figure results. OM micrographs of the L/2 zone section confirm the presence of two different textured domains at  $\approx -20^\circ$  and  $\approx 20^\circ$  from the direction of H. SEM micrographs exhibit a large amount of 211 precipitates which have three specific sizes, 3  $\mu\text{m}$ , 10  $\mu\text{m}$ , and 30  $\mu\text{m}$  respectively.



Figure 3. TEM Bright field image

Figure 3 shows an example of 211 precipitates. The matrix present on the figure has the same orientation in the whole area of the micrograph, while 211 precipitates have different orientations. It is important to note the large amount of defects around the small 211 particles. These 211/123 resulting interfaces should act as pinning centers.

### REFERENCES

1. D. Braithwaite, D. Bourgault, A. Sulpice, J. M. Barbut, R. Tournier, I. Monot, M. Lepropre, J. Provost, G. Desgardin, *Journ. Low Temp. Phys.*, **91**, 1, (1993).
2. R.L. Meng, C. Kinalidis, Y.Y. Sun, L. Gao, Y.K. Tao, P.H. Hor and C.W. Chu, *Nature* **345**, 326-328 (1990).
3. P.J. McGinn, M.A. Black, and A. Valenzuela, *Physica. C* **156**, 57-61(1988).
4. J. M. Barbut, M. Barrault, F. Boileau, M. Ingold, D. Bourgault, P. De Rango, R. Tournier, to be published in *J. Phys. III*, (1994).
5. L. G. Schulz, *J. A. P.*, **20**, 1030, (1949).